Supporting Information

Tunable Grain Orientation of Chalcogenide Film and Its Application for Second Harmonic Generation

Yun Meng[1,2,4], Jitendra K. Behera[3], Shancheng Wang[4], Minghui Jiang[1,2], Jincheng Lin[1,2], Jingsong Wei[1,2], Yang Wang[1,2]*, Tun Cao[3,]* and Yi Long[4,]*

[1]Laboratory of Micro-Nano Optoelectronic Materials and Devices, Key Laboratory of Materials for High-Power Laser, Shanghai Institute of Optics and Fine Mechanics, Chinese Academy of Sciences, Shanghai 201800, China
[2]Center of Materials Science and Optoelectronics Engineering, University of Chinese Academy of Science, Beijing 100080, China
[3]School of Optoelectronic Engineering and Instrumentation Science, Dalian University of Technology, Dalian, 116024, China
[4]School of Materials Science and Engineering, Nanyang Technological University, 50 Nanyang Avenue, Singapore 639798, Singapore

Corresponding Authors: ywang@siom.ac.cn; caotun1806@dlut.edu.cn; longyi@ntu.edu.sg

1. Femtosecond laser for SHG measurement

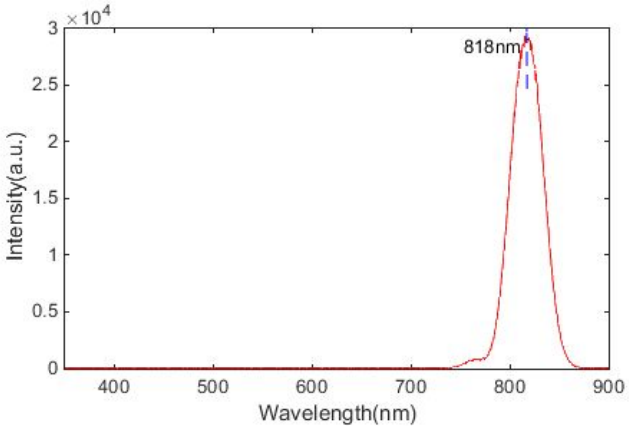

Figure S1 The output spectrum of the femtosecond laser source.

The center wavelength and linewidth of the femtosecond laser are about 818nm and 40 nm (FWHM) respectively, as shown in Figure S1.

2. FDTD simulation of the orientation-dependent transmittance

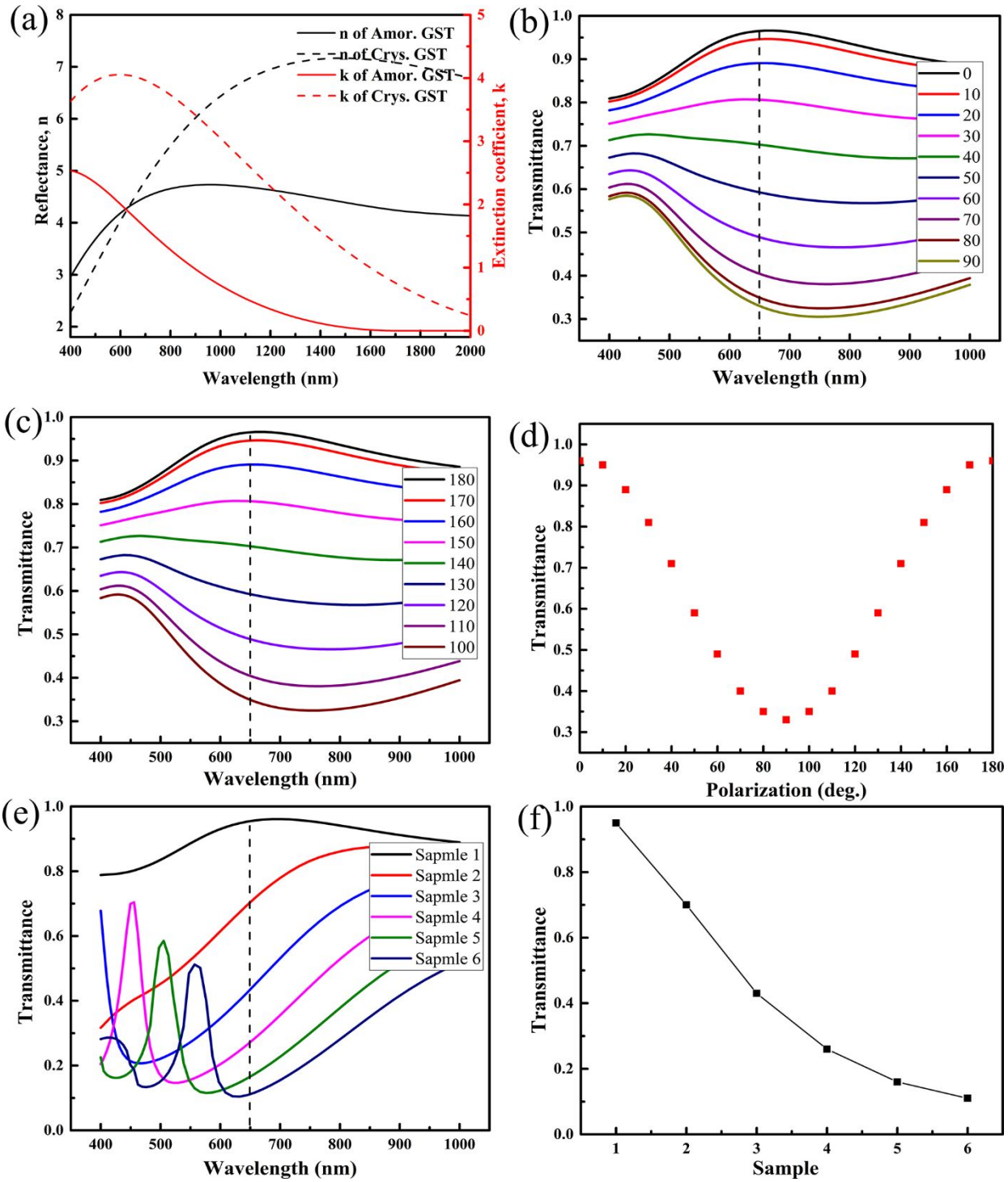

Figure S2 (a)The optical constant of GST used for simulation; (b)(c) simulated transmission spectra of the oriented GST grains at different polarization directions. (d)The polarization-dependent transmittance at 650nm. (e)Simulated transmittance changes in the samples with different grain sizes; (f)Summarized transmittance changes at the wavelength of 650 nm.

The FDTD method was used to simulate how orientated grains influence

transmittance. A uniform 2 nm FDTD square mesh was used in the simulation. The complex refractive index of the GST film for both the amorphous and crystalline states are presented in Figure S2a, which was obtained from a 35 nm thick GST film on a silicon substrate by using an ellipsometer. The length to width ratio of the grain is set as 1.5:1, and the distance of two adjacent grains is 100 nm. The width of the grains in Sample 1 to Sample 6 is 50 nm, 100 nm, 150 nm, 200 nm, 250 nm and 300 nm, respectively. The transmittance at different polarization angles (from 0 degree to 180 degree) of Sample 1 was shown in Figure S2b and Figure S2c. It was found that the transmittance undergoes a sinusoidal periodic variation when the polarization angle of the pump laser (@650 nm) rotates 180 degrees, as summarized in Figure S3d. The grain size-dependent transmittance of the six samples was studied as shown in Figure S2e. The transmittance decrease with the increase of the grain size obviously (Figure S2f).

3. SHG measurement during laser-induced crystallization

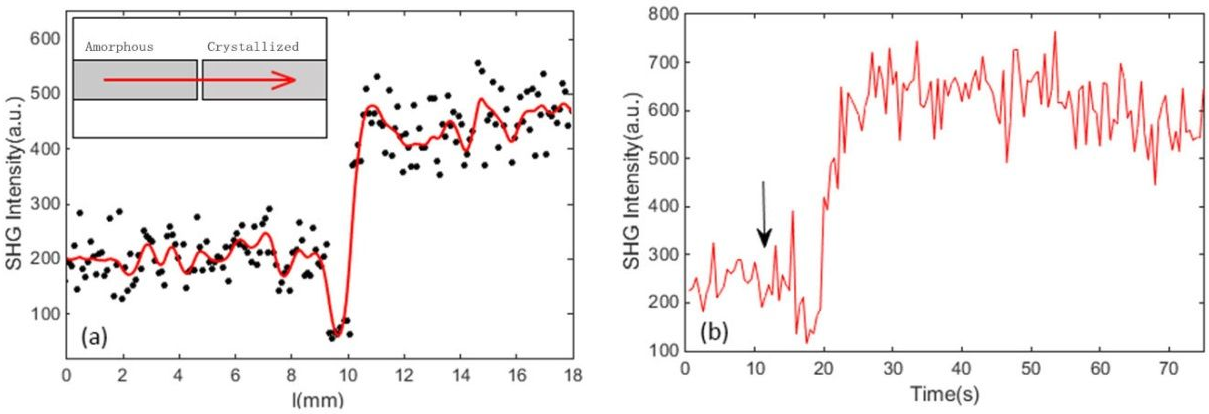

Figure S3(a) SHG intensity changes between the amorphous area and crystallized area of the film; (b) real-time SHG variations of the film induced by successive laser pulses.

In this work, we found that the reflected SHG signal can work as an optical parameter to characterize the crystallization state of phase change materials. As shown in Figure S3a, the intensity of SHG signals was enhanced when the testing spot is moved from the amorphous area to the crystallized area. Then we measured the real-time SHG variations when the amorphous film was irradiated by successive laser pulses. As shown in Figure S3b, the SHG intensity was increased during laser irradiation, indicating that crystalline grains were formed gradually.

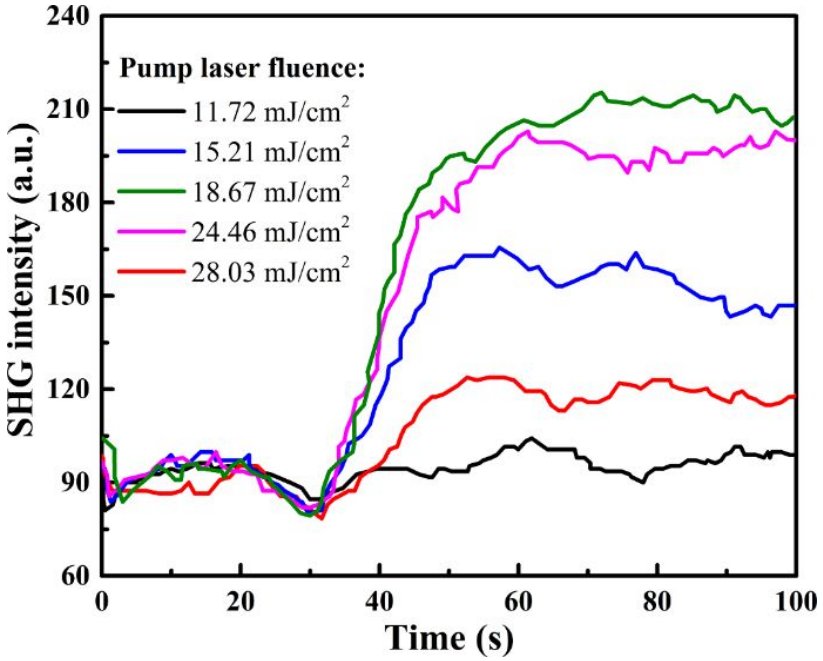

Figure S4 The variation of SHG intensity of as-deposited amorphous GST thin films during picosecond laser irradiation at different fluences.

The variation of SHG intensity of GST thin films during picosecond laser irradiation at different fluences was shown in Figure S4. It can be seen that the SHG intensity increases gradually with the laser irradiation time (pulse numbers) and reaches the maximum. An obvious threshold effect can be observed. When the

fluence of the pump laser is low (11.72 mJ/cm^2), the SHG intensity kept almost unchanged during laser irradiation. With the increase of laser fluences (15.21 and 18.67 mJ/cm^2), the films were crystallized to a higher degree, which corresponds to a larger final value of SHG intensity. The final value of SHG decreases with a further increase of fluences (24.46 and 28.03 mJ/cm^2). This is because part of the irradiated area begins to be ablated when the fluence reaches the damage threshold.

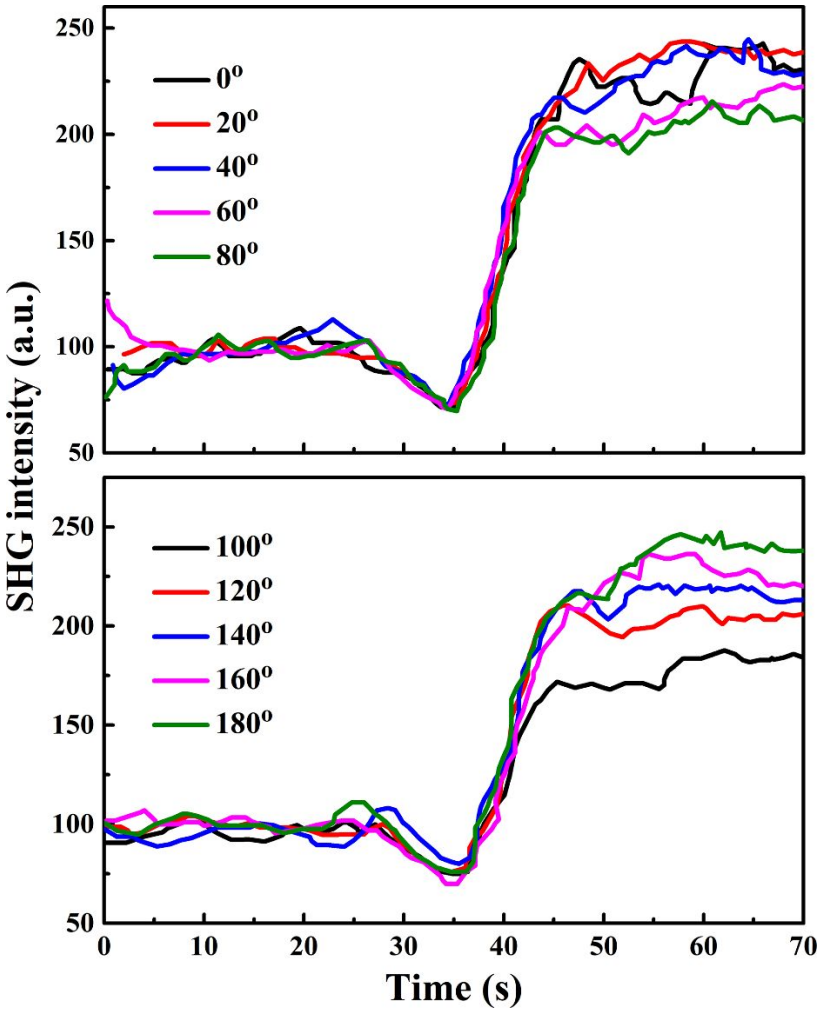

Figure S5 The change of SHG intensity of as-deposited amorphous GST thin films during laser-induced crystallization by pump laser with different polarization angles.

The SHG intensity is very weak before the incident of the pump laser. After pumping, the signal gradually decreases a little in the first 15 seconds and then starts

to rise rapidly to a higher value, which changes with the polarization angle of the pump laser. After the pump light stops, it can still stay at a high value. This shows that the orientation of the grains is modulated by the polarization angle of the pump light. The orientation of the grains produced by the laser-induced crystallization with different polarization angles is also different. The change of the angle between the grain orientation and the polarization direction of the probe laser results in the change of SHG intensity.

By averaging the values after stabilization (50 s-70 s in Figure S5), the relationship between SHG intensity and polarization angle of pump laser can be obtained, as shown in Figure 3d.

4. Calculation of the orientation degree

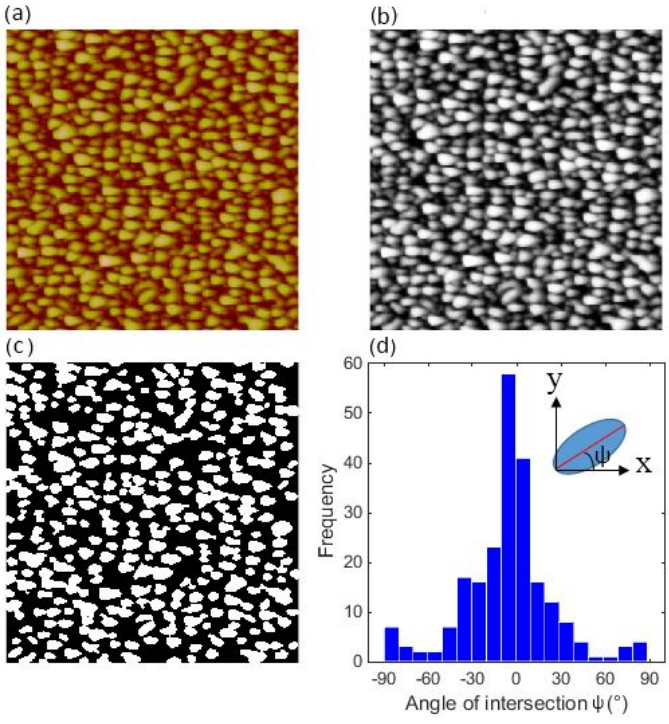

Figure S6 Process of the AFM images of the $Ge_2Sb_2Te_5$ films after irradiation by polarized

picosecond laser pulses. (a) Original image, (b) grey-scale image after de-noising and image enhancement, (c) binary image, (d) angular distribution of the crystal grains.

To analyze the orientation of crystal grains induced by polarized picosecond laser pulses, the morphological structure of the sample was further studied by the image processing tool (Regionprops toolbox of MATLAB), as shown in Figure S6. The angle of intersection (ψ) between the long axis of an ellipse-like grain and the X-axis (horizontal line of the figure) is measured for each grain in this area (9×9 μm) and the angular distribution can be obtained. Orientation degree, which is generally expressed by orientation function: $F = \frac{1}{2}(3\overline{\cos^2 \Psi} - 1)$.

The shape of grains is not needed to be very elliptical. For example, a tapered grain can be fitted to an ellipse with the same standard second-order central moment. The long axis of the grain is defined as the long axis (y-axis) of the fitted ellipse. Fitting and measurement can be fulfilled with the image processing tool mentioned above. Figure S7 shows the angular distributions of the crystal grains during reversible orientation modulation.

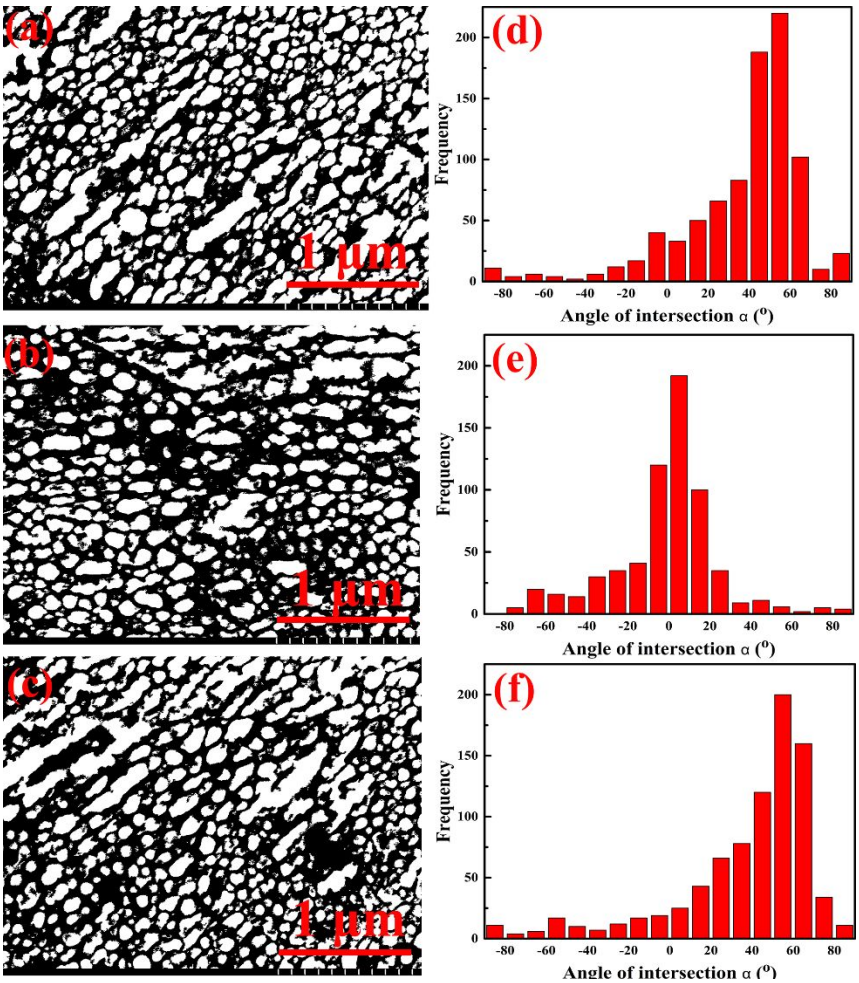

Figure S7. (a)(b)(c), Binary images of selected areas in recording spots after processing; (c)(f)(i) corresponding binary images after processing, (d)(e)(f) angular distributions of the crystal grains. Laser irradiation time: 30s, laser fluence: 18.67 mJ/cm^2.